

Ordering dynamics in the voter model with aging

Antonio F. Peralta, Nagi Khalil, and Raúl Toral
*IFISC (CSIC-UIB), Instituto de Física Interdisciplinar y Sistemas Complejos,
Campus Universitat de les Illes Balears, E-07122 Palma de Mallorca, Spain*

The voter model with memory-dependent dynamics is theoretically and numerically studied at the mean-field level. The “internal age”, or time an individual spends holding the same state, is added to the set of binary states of the population, such that the probability of changing state (or activation probability p_i) depends on this age. A closed set of integro-differential equations describing the time evolution of the fraction of individuals with a given state and age is derived, and from it analytical results are obtained characterizing the behavior of the system close to the absorbing states. In general, different age-dependent activation probabilities have different effects on the dynamics. When the activation probability p_i is an increasing function of the age i , the system reaches a steady state with coexistence of opinions. In the case of aging, with p_i being a decreasing function, either the system reaches consensus or it gets trapped in a frozen state, depending on the value of p_∞ (zero or not) and the velocity of p_i approaching p_∞ . Moreover, when the system reaches consensus, the time ordering of the system can be exponential ($p_\infty > 0$) or power-law like ($p_\infty = 0$). Exact conditions for having one or another behavior, together with the equations and explicit expressions for the exponents, are provided.

I. INTRODUCTION

Agent-based binary-state models are commonly used to study the effect that simple individual dynamical rules may have on the collective behavior of a system. Typical examples include modeling the spreading of diseases [1, 2], the time evolution of the number of speakers of a determined language [3–6], the evolution of prices in financial markets [7–13], or the dynamics of opinion formation in a population of individuals [14–16]. As a prominent case of the latter, the voter model [17–19] and its variants thereof [20], by which an agent adopts with some probability the state of a randomly chosen neighbor, are widely used when the mechanism at hand is that of imitation. Beyond its potential applications, the voter model has become a paradigm in the field of non-equilibrium statistical physics. It is defined by very simple rules, and explicit solutions can be given in some particular cases, yet it is capable of showing very rich behavior, including phase transitions, characterized by critical exponents, power-law correlations, finite-size scaling, tricritical behavior, etc. [21, 22]. Recent studies of the voter model include the effect of a network structure [23, 24], non-linear or group interactions [25–31], the effect of zealots [32] and contrarians [33].

A fundamental aspect of the agent-based binary-state models is the memory the constituents of the system have [34], and how this affects the dynamical rules that define the model. A clear example is the framework of non-Poissonian infection processes in epidemic spreading [35–37], where the infection of an individual depends on the times each one of its neighbors became infected [38]. This is because the rate at which one transmits a disease is not independent of the time one has been infected. In most cases of binary-state models a Markovian assumption is postulated which implies that the probability of changing state is independent of the past history of events of the individuals, that is to say neglecting memory effects by including Poissonian processes. This is of course a simplification that can be justified in many phenomena and it makes a lot easier the mathematical treatment [39, 40], but it may be lacking of realistic features in other cases. In this context, one of the objectives of the present work is to provide a consistent mathematical description of the voter model including memory effects, namely by making the probability of changing opinion of agents to depend on their age or time elapsed until their last update [41, 42].

One of the main questions addressed by the voter model is whether the imitation rule leads to a situation of consensus, with all agents (or at least, a significant majority) adopting the same value of the binary state [43–45]. The answer to this question is sometimes counter-intuitive. Although it would appear, for example, that an increase in the connections amongst the agents should favor consensus, a detailed analysis shows that for an effective dimensionality of the connectivity network greater than two, the system is not able to sustain a consensus state in the thermodynamic limit. The problem has been also addressed when including memory effects. Stark et. al [42] introduced increasing inertia, otherwise known as “aging”, as a mechanism that reduces the probability of an agent to copy the state of another one. Again, it would seem naively that reducing the number of interactions amongst agents should impede the reaching of consensus, but it was shown that exactly the opposite happens, namely the consensus is reached more easily in such an scenario of aging. In a recent paper by some of us [46, 47], it was shown that the inclusion of aging in the noisy version of the voter model [7, 48, 49] induces a state of imperfect consensus that remains in the thermodynamic limit. Another study of the noiseless voter model [41] focused on the distribution of the time between individual changes of states $C(t)$, which in turn is related with the activation probability p_i , or the age-dependent

probability of interaction. The conclusion of [41], sustained from the analysis of extensive numerical simulations, was that a particular functional form of $p_i \sim \beta/i$ induces a power-law dependence $C(t) \sim t^{-\beta}$, which has been observed in real datasets, for example in human communications [50, 51]. This power law is similar to the ones observed in the approach to consensus in low-dimensional lattices, but it shows a strong dependence on the details of the activation probability. The main objective of this paper is to analyze this problem and to derive the relations in [41, 42], among others, from an analytical point of view. We also aim to give a well constructed theoretical framework for aging, which has been studied together with network structure in several recent works [52–54] but mainly computationally, due to difficulties encountered in the mathematical description.

The outline of the paper is as follows. In section II we introduce the voter model including memory effects. Two specific forms of the activation probability, rational and exponential functions of the age, are considered which depend on several parameters, so as to cover phenomenology observed in the literature. Section III includes a summary of the main results present in the literature about dynamical behavior of the system close to the absorbing states. In section IV the dynamical equations of the mean fraction of agents with a given state and age are obtained under a mean field description and its steady-state analysed. Section V contains the main results of the work. First, a closed set of integro-differential equations describing the system close to the absorbing states is derived. Second, an approximate analysis of the previous description is carried out, providing explanation to the numerical findings. Complementary results are given in A and B. Finally, section VI includes a summary of the main results.

II. MODEL

The voter model implements in arguably the simplest way the herding mechanism for the evolution of binary state systems. In the original version one considers a system formed by N individuals or agents. Agents are located in the nodes of a network and are connected by undirected, bidirectional, links. Two connected individuals are said to be “neighbors”. The network is single connected, meaning that every node can be reached from any other node by a sequence of links. Each individual $k = 1, \dots, N$ holds a binary-state (spin) variable $s_k = \pm 1$. Several interpretations can be given to this binary variable, but its exact meaning does not concern us in this paper. For example, the voter model or variants of it have been used to represent the optimistic/pessimistic state of a stock market broker [7], the language A/B used by a speaker [3, 6], or the direction of the velocity right/left in a one-dimensional model of active particles [55]. Those variables evolve over time by the following (stochastic) rules:

- (i) An individual k is selected at random amongst the N possibilities.
- (ii) The selected individual copies the state $s_k = s_{k'}$ of another individual k' chosen also at random between the set of neighbors of k .

In this sequential updating scheme, every time an individual is chosen for updating, time t increases by one unit, while N updates constitute one Monte Carlo step (MCS).

In the aging version of the voter model the above rules are modified such that the herding mechanism occurs only with an *activation probability* p_{i_k} that depends on the *internal age* i_k of the selected individual. The internal age $i_k = 0, 1, 2, \dots$ of individual k stands for the number of update attempts elapsed since its last change of state.

More explicitly, the model is reproduced in the simulations by modifying the last step as follows:

- (ii) The selected individual copies **with probability** p_{i_k} the state $s_k = s_{k'}$ of another individual k' chosen at random between the set of neighbors of k . If the selected individual changes state $s_k \rightarrow -s_k$, then its internal age resets to zero $i_k \rightarrow 0$; otherwise it increases in one unit $i_k \rightarrow i_k + 1$. Initially, all internal ages are set to zero.

The standard (no aging) voter model is recovered taking $p_i = 1$. Here, for the sake of concreteness and mathematical treatment, we have considered the following two functional forms for the activation probability:

- 1.- The first functional form is a rational function of the age,

$$p_i = \frac{p_\infty i + p_0 c}{i + c}, \quad i = 0, 1, 2, \dots \quad (1)$$

where $p_0, p_\infty \in [0, 1]$ and $c > 0$ are constants. If $p_0 > p_\infty$, the probability of interaction decreases with age, a typical aging situation. The opposite occurs if $p_0 < p_\infty$, as the activation probability increases with age. This can be interpreted as “anti-aging” or “rejuvenating” where as nodes get older they become more prone to change state. This aging form, with $p_\infty = 0$, is basically the form considered in [41] and that has been shown to induce features observed in several real-world systems, such as power-law inter-event time distributions. If $p_0 = 1$ and $p_\infty > 0$, this reproduces qualitatively the form used in Ref. [42]. In that paper, the activation probability p_i , equivalent to $1 - \nu_i$ with ν_i being the “inertia”, decreases linearly from $p_0 = 1$ up to a final constant, non-null value p_∞ , but at a finite value of i .

2.- The second form we adopt for mathematical simplicity is an exponential dependence of the age,

$$p_i = (p_0 - p_\infty)\lambda^i + p_\infty, \quad i = 0, 1, 2, \dots \quad (2)$$

with the same meaning as before for p_0 and p_∞ , and $\lambda < 1$ is a parameter.

III. DYNAMICAL BEHAVIOR. ABSORBING STATES

When one individual changes its state after copying the state of one of its neighbors, it might occur that it decreases the total number of neighbors with which it shares the same state. Therefore, a question of interest is whether by iteration of the dynamical rules a ‘‘consensus’’, or fully ordered, state in which all agents share the same state, either $+1$ or -1 , is finally achieved. One can argue that the stochastic rules permit eventually to reach any possible configuration of states. Therefore, when any of the particular consensus states $s_k = +1, \forall k$ or $s_k = -1, \forall k$ is reached, then there can not be further evolution and the dynamics stops. It seems, though, that the ultimate fate of the system is to reach consensus, with all nodes sharing the same value. While this is certainly true for any system with a finite number N of agents, it is interesting to analyze the way the consensus state is reached and the dependence with system size of the average time to reach that state. Two different measures have been introduced to study the approach to order: the magnetization $m(t) = N^{-1} \sum_{k=1}^N s_k(t)$ that takes values $m = \pm 1$ in the ordered states, and the density $\rho(t)$ of active links, defined as the fraction of links that join nodes in different states. In the ordered states, the magnetization can be $m = +1$ or $m = -1$, while $\rho = 0$ in both absorbing states. The existence of absorbing states then ensures that $\lim_{t \rightarrow \infty} m(t) = \pm 1$ and $\lim_{t \rightarrow \infty} \rho(t) = 0$ for a finite system.

There is a significant difference between the aging and non-aging versions of the model. In the non-aging version the approach to the absorbing state depends crucially on the spatial dimension d . If $d > 2$ it is observed that the density of active links[?] has a fast transient to a plateau value ρ^* (for $d \rightarrow \infty$, i.e. all to all connectivity, $\rho^* = \rho(0)$) and it oscillates around it until a large fluctuation brings the system to the absorbing state $\rho = 0$ at a time T . This time is a stochastic variable whose mean value scales as $\langle T \rangle \sim N$ for $d > 2$, see also [56] where the probability distribution of T is obtained for $d \rightarrow \infty$. Therefore, larger systems stay longer in an active state until a large fluctuation brings them to the absorbing state. As we take the thermodynamic limit $N \rightarrow \infty$, it is $T \rightarrow \infty$ and the system does not order at all in a finite time. If we average over initial conditions and realizations of the dynamics, we find an exponential decay $\langle \rho(t) \rangle = \rho^* e^{-t/\tau}$, with $\tau \propto \langle T \rangle$. As mentioned, in the thermodynamic limit when $\langle T \rangle = \infty$, we obtain $\langle \rho(t) \rangle = \rho^*$, or absence of order. If we take first the limit $t \rightarrow \infty$ and then the limit $N \rightarrow \infty$ we obtain otherwise $\lim_{N \rightarrow \infty} \lim_{t \rightarrow \infty} \langle \rho(t) \rangle = 0$. If the spatial dimension is $d \leq 2$ the decay to the absorbing state occurs very differently. One does not observe that $\rho(t)$ fluctuates around a plateau value, but rather $\rho(t)$ decreases on average for any realization even for large system sizes. As a consequence, in the thermodynamic limit, it is predicted that $\lim_{t \rightarrow \infty} \lim_{N \rightarrow \infty} \langle \rho(t) \rangle = 0$. The exact time dependence depends on the dimension as $\lim_{N \rightarrow \infty} \langle \rho(t) \rangle = (\log t)^{-1}$ for $d = 2$ and $\lim_{N \rightarrow \infty} \langle \rho(t) \rangle = t^{-1/2}$ for $d = 1$ [43–45].

The phenomenology in the aging version was described in [41] for particular forms of the activation probability. It was observed that if p_i follows a similar dependence as given by Eq. (1) with $p_\infty = 0$, then the approach to the absorbing states is always described by a power law $\lim_{N \rightarrow \infty} \langle \rho(t) \rangle = t^{-\beta}$, even for large spatial dimensions. Furthermore, in a fully-connected network it was observed numerically that the exponent β of the power-law decay agreed within the numerical accuracy with the parameter $b = p_0 c$ of Eq. (1)[?]. This indicates that in the presence of aging, the system always orders, contrarily to the non-aging version. In this paper we offer an explanation of this behavior.

IV. THE DYNAMICAL EQUATIONS

We now derive the mean-field dynamical equations of our stochastic process, as defined in section II. In the derivation we restrict ourselves to the all-to-all (or fully connected) network in which all nodes are neighbors. The mathematical description in the case of a more complex network structure in the interactions between nodes is a further complication [23] and it is left for future studies [53, 54]. In the all-to-all setup, all the information needed to implement the stochastic update rules is contained in the set $S \equiv \{n_i^\pm\}_{i=0}^\infty$ of the numbers of individuals with internal age i in states ± 1 , [42]. The global variables for the total number of up and down spins are $n = \sum_{i=0}^\infty n_i^+$ and $N - n = \sum_{i=0}^\infty n_i^-$. Note, however, that not all variables of the state S are independent, since $\sum_{i=0}^\infty (n_i^+ + n_i^-) = N$. Hence, it is useful to consider an alternative representation of the system in terms of independent variables, for instance by using the variable n and obviating n_0^\pm , as $S_n \equiv (n, \{n_i^+\}_{i=1}^\infty, \{n_i^-\}_{i=1}^\infty) = (n, n_1^+, n_2^+, \dots, n_1^-, n_2^-, \dots)$. In this representation n_0^\pm are given by $n_0^+ = n - \sum_{i=1}^\infty n_i^+$ and $n_0^- = N - n - \sum_{i=1}^\infty n_i^-$.

In order to derive the dynamical equations of the global state of the system S_n we must include with their respective probabilities all events that induce changes in S_n . Every time an individual changes its state or age, there is a change in the set of variables S_n . The change can occur in different ways and with different probabilities. We now spell in detail the possibilities and their effects on the variables.

(1) Consider that at time t the chosen individual k is in state $s_k = +1$ and has age $i_k = i$ and that as a result of the interaction it switches to $s_k = -1$ and, hence, its internal age is reset to $i_k = 0$. The probability of this event is equal to the probability, $\frac{n_i^+}{N}$, of choosing an individual with age i and state $+$, multiplied by the age-dependent probability, p_i , that it activates the copying (herding) mechanism, and multiplied by the probability $\frac{N-n}{N}$ that the randomly selected neighbor is in the opposite state. Altogether, the probability is $\frac{n_i^+}{N} p_i \frac{N-n}{N} \equiv \frac{1}{N} \Omega_{1,i}$. When the switching of state occurs, if $i > 0$ we have $n_i^+ \rightarrow n_i^+ - 1$ and $n \rightarrow n - 1$, while if $i = 0$ the only change is $n \rightarrow n - 1$.

(2) This is similar to the previous case but now the chosen individual is initially in state $s_k = -1$. The probability of switching is $\frac{n_i^-}{N} p_i \frac{n}{N} \equiv \frac{1}{N} \Omega_{2,i}$. When the switching of state occurs, if $i > 0$ we have $n_i^- \rightarrow n_i^- - 1$ and $n \rightarrow n + 1$, while if $i = 0$ the only change is $n \rightarrow n + 1$.

(3) Consider that at time t the chosen individual k has $s_k = +1$ and age $i_k = i$, but that now it keeps its current state $s_k = +1$. This event happens with a probability equal to the probability of choosing an individual in state $+1$ with age i , $\frac{n_i^+}{N}$, multiplied by the probability that it does not switch, which can arise either because the copying mechanism was not activated, with probability $1 - p_i$, or it was activated but the selected neighbor was in the same state, with probability $p_i \frac{n_i^+}{N}$. Altogether, the probability is $\frac{n_i^+}{N} (1 - p_i + p_i \frac{n_i^+}{N}) \equiv \frac{1}{N} \Omega_{3,i}$. In this case the variables change as $n_i^+ \rightarrow n_i^+ - 1$ and $n_{i+1}^+ \rightarrow n_{i+1}^+ + 1$ if $i > 0$ and $n_1^+ \rightarrow n_1^+ + 1$ if $i = 0$.

(4) Finally, we consider a similar case to the previous one but the chosen individual $s_k = -1$ keeps its state. The switching probability is now $\frac{n_i^-}{N} (1 - p_i + p_i \frac{N-n}{N}) \equiv \frac{1}{N} \Omega_{4,i}$. The changes in the state S_n are $n_i^- \rightarrow n_i^- - 1$, $n_{i+1}^- \rightarrow n_{i+1}^- + 1$ if $i > 0$ and $n_1^- \rightarrow n_1^- + 1$ if $i = 0$.

If time is measured in MCS, the rates (probability per unit time) of the four possible processes are

$$\Omega_{1,i} = n_i^+ \beta_i (1 - n/N), \quad \Omega_{2,i} = n_i^- \beta_i (n/N), \quad (3)$$

$$\Omega_{3,i} = n_i^+ \alpha_i (1 - n/N), \quad \Omega_{4,i} = n_i^- \alpha_i (n/N), \quad (4)$$

where $\beta_i(x) = p_i x$ and $\alpha_i(x) = 1 - \beta_i(x)$, thus $\Omega_{1,i} + \Omega_{3,i} = n_i^+$, $\Omega_{2,i} + \Omega_{4,i} = n_i^-$.

This derivation has considered a discrete time process in the limit of a large number of individuals. It is also possible to consider from the beginning a continuous time process in which an agent of age i and state $s = +1$ has a rate $\beta_i(1 - n/N)$ of switching state and set its internal age to 0, and a rate $\alpha_i(1 - n/N)$ of increasing its internal age keeping the state; similarly an agent of age i and state $s = -1$ has a rate $\beta_i(n/N)$ of switching state and set its internal age to 0, and a rate $\alpha_i(n/N)$ of increasing its internal age and keep the state.

Following standard techniques [57–59], we could derive a master equation for the probability $P(S_n, t)$ of having state S_n at time t , with the set of rates and changes in the variables explained before. As we restrict ourself to average values in this paper, we will only obtain the evolution equations for the ensemble average of the fraction of nodes with a given state and age $x_i^\pm = \langle n_i^\pm \rangle / N$, as well as for $x = \langle n \rangle / N$. The time evolution of the average values can be computed as a weighted sum of all the rates that contribute to its variation, the weights being the variation of the regarded variable in that process [59]. Using the standard mean-field approximation [58] which neglects correlations as $\langle n_i^\pm n \rangle \simeq \langle n_i^\pm \rangle \langle n \rangle$ we end up with a closed but infinite system of equations:

$$\frac{dx_i^+}{dt} = -x_i^+ + x_{i-1}^+ \alpha_{i-1} (1 - x), \quad i \geq 1, \quad (5)$$

$$\frac{dx_i^-}{dt} = -x_i^- + x_{i-1}^- \alpha_{i-1} (x), \quad i \geq 1, \quad (6)$$

$$\frac{dx}{dt} = \sum_{i=0}^{\infty} x_i^- \beta_i (x) - \sum_{i=0}^{\infty} x_i^+ \beta_i (1 - x). \quad (7)$$

Similar equations were obtained in Ref. [42, 46]. In these equations, variables x_0^\pm , whenever they appear, should be

expressed in terms of the independent variables,

$$x_0^+ = x - \sum_{i=1}^{\infty} x_i^+, \quad x_0^- = 1 - x - \sum_{i=1}^{\infty} x_i^-. \quad (8)$$

The explicit time evolution of these variables is

$$\frac{dx_0^+}{dt} = -x_0^+ + \sum_{i=0}^{\infty} x_i^- \beta_i(x), \quad (9)$$

$$\frac{dx_0^-}{dt} = -x_0^- + \sum_{i=0}^{\infty} x_i^+ \beta_i(1-x). \quad (10)$$

By equating all time derivatives to zero, we can identify the steady-state solutions for the mean-field description. From Eqs. (5,6,8) we find

$$x_{i,\text{st}}^+ = \frac{x_{\text{st}}}{f(x_{\text{st}})} \prod_{k=0}^{i-1} \alpha_k(1-x_{\text{st}}), \quad x_{i,\text{st}}^- = \frac{1-x_{\text{st}}}{f(1-x_{\text{st}})} \prod_{k=0}^{i-1} \alpha_k(x_{\text{st}}), \quad i \geq 0, \quad (11)$$

where

$$f(x) \equiv \sum_{i=0}^{\infty} \prod_{j=0}^{i-1} \alpha_j(1-x), \quad (12)$$

and the convention $\prod_{j=0}^{-1} \alpha_j \equiv 1$. Obviously, the validity of these relations require that the series Eq. (12) defining $f(x)$ is convergent. This is certainly not the case for $x = 1$, as $f(x = 1) = \infty$ always. As we will see, another case in which the series might diverge occurs when $p_{\infty} = 0$, when d'Alembert's criterion does not ensure convergence as $\lim_{i \rightarrow \infty} \alpha_i(x) = 1$. Using Eqs. (7,9,10) in the steady state, one obtains easily $x_{0,\text{st}}^+ = x_{0,\text{st}}^-$, or

$$\frac{x_{\text{st}}}{f(x_{\text{st}})} = \frac{1-x_{\text{st}}}{f(1-x_{\text{st}})}. \quad (13)$$

The solutions to this equation provide the possible steady-state values of $x_{\text{st}} = \langle n \rangle / N$ and those values of x_{st} determine the other quantities, through Eqs. (11). Note that $x_{\text{st}} = 1/2$ is always a trivial solution that corresponds to a symmetric steady state, with the same mean number of nodes with a given age having opposite states $x_{i,\text{st}}^+ = x_{i,\text{st}}^-$ for $i \geq 0$. In any case, the steady-state solutions describe situations where $x_{i,\text{st}}^{\pm}$ are decreasing functions of the age. Note also that $x_{\text{st}} = 0, 1$ are always steady state solutions (absorbing states) of the dynamics, and indeed satisfy Eq. (13) as $f(x \rightarrow 1) \rightarrow \infty$ and $f(x \rightarrow 0) \rightarrow \text{constant}$.

For the particular case $p_i = p, \forall i$, we obtain the function $f(x) = 1/(p(1-x))$. Eq. (13) is satisfied for any x_{st} and, in fact, it can be shown that Eq. (7) becomes $\frac{dx}{dt} = 0$ and, hence, $x_{\text{st}} = x(0)$. This is the behavior of the non-aging voter model in the thermodynamic limit that was described before. If $x_{\text{st}} \neq 0, 1$, the distribution of ages in this steady state follows a geometric distribution: $x_{i,\text{st}}^+ = px_{\text{st}}(1-x_{\text{st}})(1-p(1-x_{\text{st}}))^i$ and $x_{i,\text{st}}^- = px_{\text{st}}(1-x_{\text{st}})(1-px_{\text{st}})^i$. For $x_{\text{st}} = 0, 1$, see section V.

For the activation probabilities Eq. (1), one finds[?]

$$f(x) = 1 + (1-p_0(1-x)) {}_2F_1 \left[1, 1 + c \frac{1-p_0(1-x)}{1-p_{\infty}(1-x)}; 1+c; 1-p_{\infty}(1-x) \right], \quad (14)$$

where ${}_2F_1[\alpha, \beta; \gamma; x]$ is the Gauss hypergeometric function. This function, and hence the series Eq. (12), is always convergent for $p_{\infty}(1-x) > 0$. If $x = 1$, we already know that the series is divergent. If $p_{\infty} = 0$, the series diverges whenever $x \geq 1 - 1/(cp_0)$. Although these divergences may be problematic in the case $p_{\infty} = 0$, one can still study Eq. (13) as a limit $p_{\infty} \rightarrow 0$ or, alternatively regularize the sum Eq. (12) with a cut-off $\sum_{i=0}^M (\dots)$ and study the dependence with M [?]. We checked that the predicted behavior of the fixed points of Eq. (13) in all cases is correct. In Figure (1a) we plot $R(x) \equiv \frac{1-x}{f(1-x)} - \frac{x}{f(x)}$ in a case of aging $p_0 > p_{\infty}$ and anti-aging $p_0 < p_{\infty}$. We find in both cases that $R(x_{\text{st}}) = 0$ provides the three mentioned fixed points, $x_{\text{st}} = 0, 1/2, 1$. We also hypothesize that the sign of $R(x)$ determines the stability or the direction of movement of x , $\frac{dx}{dt}$, thus for aging we expect the symmetric solution $x_{\text{st}} = 1/2$ to be unstable and the absorbing states $x_{\text{st}} = 0, 1$ stable and the other way around for anti-aging [60]. The time-dependence and ordering dynamics depending on the form of p_i is studied in detail in the next section.

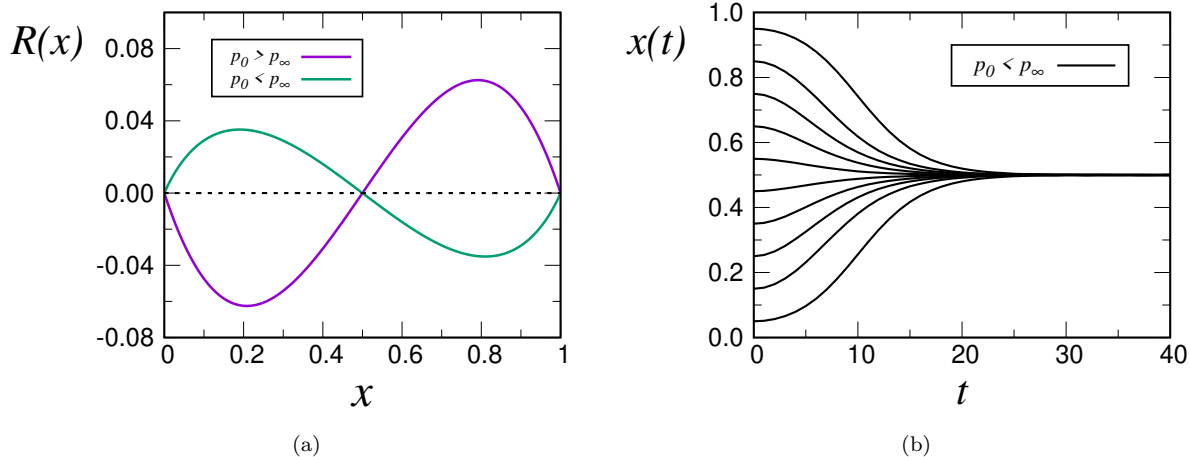


FIG. 1. In the left panel we show $R(x) \equiv \frac{1-x}{f(1-x)} - \frac{x}{f(x)}$ using Eq.(1) for the case of aging $p_0 = 0.9$, $p_\infty = 0.1$ and $c = 1$, purple line, and for anti-aging, $p_0 = 0.1$, $p_\infty = 0.9$ and $c = 1$, green line. The right panel shows trajectories $x(t)$ coming from numerical simulations of anti-aging, $p_0 = 0.5$, $p_\infty = 1$ and $c = 1$, with different initial conditions $x(0)$ and $N = 10^5$ agents, averages were performed over 10^2 trajectories.

V. ORDERING DYNAMICS

It is clear from the rules of the process that the absorbing states $x(t) = 0$ and $x(t) = 1$ must be solutions of the dynamical equations in all cases, whatever the particular form of p_i . We now discuss these solutions. For the sake of concreteness we consider only the $x = 0$ absorbing state, but an equivalent analysis could be performed at $x = 1$ as well. Consider, then, that the system is at $x = 0$ at time $t = 0$ with all internal ages set to 0. As there are no nodes in the $+1$ state, the herding mechanism implies that a selected node can never switch state to $+1$ and will remain in the -1 state, hence increasing its internal age in one unit according to the rules of the model. Therefore we have $x_i^{+(0)}(t) = 0$, $x^{(0)}(t) = 0$, and thus Eq. (10) reduces to $\frac{dx_0^{-(0)}}{dt} = -x_0^{-(0)}$, or $x_0^{-(0)}(t) = e^{-t}$, where the superscript (0) indicates that those values are valid at the absorbing state $x = 0$. The solution of Eqs. (6) with $x = 0$ (implying $\alpha_j(0) = 1$) and the above mentioned initial conditions can be readily found as

$$x_i^{-(0)}(t) = e^{-t} \frac{t^i}{i!}, \quad i \geq 0, \quad (15)$$

which indicates that the distribution of internal ages in the population follows a Poisson distribution with $\langle i \rangle = \sigma_i^2 = t$. We now study the stability of this solution.

We linearize Eqs. (5,9) around the solution $x_i^{\pm(0)}$ at the absorbing state:

$$\frac{dx_i^+}{dt} = -x_i^+ + x_{i-1}^+(1 - p_{i-1}), \quad i \geq 1, \quad (16)$$

$$\frac{dx_0^+}{dt} = -x_0^+ + x \sum_{i=0}^{\infty} p_i x_i^{-(0)} = -x_0^+ + x \sum_{i=0}^{\infty} p_i e^{-t} \frac{t^i}{i!}. \quad (17)$$

The solution of Eq. (16) with the initial condition $x_i^+(0) = 0$, $i \geq 1$, is

$$x_i^+(t) = \prod_{k=0}^{i-1} (1 - p_k) \int_0^t \frac{(t-s)^{i-1}}{(i-1)!} e^{s-t} x_0^+(s) ds, \quad i \geq 1. \quad (18)$$

Imposing $x(t) = x_0^+(t) + \sum_{i=1}^{\infty} x_i^+(t)$, and replacing in Eq. (17) we obtain

$$x(t) = x_0^+(t) + \int_0^t G(t-s) x_0^+(s) ds, \quad (19)$$

$$\frac{dx_0^+}{dt} = -x_0^+ + L(t) \left(x_0^+ + \int_0^t G(t-s) x_0^+(s) ds \right), \quad (20)$$

with

$$G(t) = e^{-t} \sum_{i=0}^{\infty} \frac{t^i}{i!} \prod_{k=0}^i (1 - p_k), \quad (21)$$

$$L(t) = e^{-t} \sum_{i=0}^{\infty} p_i \frac{t^i}{i!}. \quad (22)$$

The integro-differential Eq. (20) has to be solved with the initial condition $x_0^+(0) = x(0)$.

A simple case in which the linearized equations (19,20) can be solved explicitly is $p_i = p$, constant. In this case we have $L(t) = p$ and $G(z) = (1 - p)e^{-pz}$, which after a tedious but straightforward calculation[?] leads to $x_0^+(t) = x(0)(p + (1 - p)e^{-t})$ and $x(t) = x(0)$, the well known solution of the voter model in the thermodynamic limit $N \rightarrow \infty$, [?].

As it follows from Eqs. (19,20) that $x'(0) \equiv \frac{dx}{dt}|_{t=0} = 0$, the stability of $x(t)$ requires to study the sign of $x''(0) \equiv \frac{d^2x}{dt^2}|_{t=0}$ which after a simple calculation, turns out to be $x''(0) = p_0(p_1 - p_0)$. Therefore, at this level, we obtain that in the anti-aging case, $p_1 > p_0$, the absorbing solution $x = 0$ is unstable, while in the aging case, $p_1 < p_0$, the absorbing solution is stable, as suggested at the end of the previous section. Since for both functional forms Eqs. (1,2) in the anti-aging case there are no other solutions than $x_{st} = 1/2$, we predict that the final state of the dynamics is that of coexistence of states. This is indeed observed in the numerical simulations, as shown in Fig. (1b).

To study in full detail the return to the absorbing state of the variable $x(t)$ we would need to solve the linearized equations (19,20). Although it does not seem to be possible to obtain their full time dependence analytically[?], simple arguments allow us to obtain the asymptotic behaviors for large t . All we need for this purpose is the asymptotic expressions of $G(t)$ and $L(t)$. We split the discussion in the cases $p_\infty = 0$ and $p_\infty > 0$, as the difference is of crucial importance.

A. Aging case, Eq. (1) with $p_\infty = 0$.

This case includes the one studied in [41] where the activation probability decayed as $p_i \sim b/i$. With our explicit expression, Eq. (1), the calculation of A leads to an asymptotic behavior valid for $p_0 < 1$,

$$G(t) \sim \frac{\Gamma(c)}{\Gamma(c(1 - p_0))} t^{-b}, \quad (23)$$

$$L(t) \sim b t^{-1}, \quad b = c p_0. \quad (24)$$

Assuming power-law dependences as $x_0^+(t) \sim t^{-\alpha}$, $x(t) \sim t^{-\beta}$ and that the integral in Eq. (20) can be approximated as $\int_0^t G(t-s)x_0^+(s)ds \sim G(t)A \sim t^{-b}$, with $A = \int_0^\infty x_0^+(s)ds$, which is justified if the time evolution of $x_0^+(t)$ is slower than that of $G(t)$, we obtain consistently $\alpha = b + 1$. Finally, using this value with Eq. (19) we get $\beta = b$. This proves that the density of nodes in the + state and, consequently, the density of active links go to zero as $x(t) \sim \rho(t) \sim t^{-b}$, explaining the numerical results of Ref. [41].

To check the previous predictions, we plot in Fig. (2) the results coming from numerical simulations for $x_0^+(t)$ and $x(t)$ for different cases of p_0 and c . As it is apparent, the figures confirm the validity of the asymptotic expansion $x(t) \sim t^{-b}$ and $x_0^+(t) \sim t^{-b-1}$, as derived theoretically. Besides the asymptotic slope, we also plot in the figures the values of $x(t)$ and $x_0^+(t)$ obtained from the numerical solution of Eqs. (19,20) using a suitable integration algorithm described in [61].

This discussion assumes that $p_0 < 1$. If $p_0 = 1$, it is $G(t) = 0$ and a direct integration of Eqs. (19,20) leads to an initial decay $x(t) \sim e^{-t^2/(2(1+c))}$, followed by an intermediate regime $x(t) \sim t^b e^{-t}$. In the numerical simulations we observe that this is followed by a crossover to the same asymptotic power-law behavior $x(t) \sim t^{-b}$. The reason why the integro-differential Eqs. (19,20) do not capture this crossover is because they are linearized. The solution of the full set of equations Eqs. (5-7) can be written $x(t) = x(0)h_1(t) + x(0)^2 h_2(t) + \dots$ with the different orders of the initial condition $x(0)$. Linearizing, we were able to find the first term $h_1(t)$. For $p_0 \neq 1$ this first term is a power law and it prevails over the rest for all times. For $p_0 = 1$ it decays exponentially and, apparently, the second order term $h_2(t) \sim t^{-b}$ is a power law. Thus for sufficiently large times $t > t^*$ it can happen that $x(0)h_1(t) < x(0)^2 h_2(t)$.

We now consider $x_i^+(t)$ for $i \geq 1$. The kernel $\frac{(t-s)^{i-1}}{(i-1)!} e^{s-t}$ inside the integral of Eq. (18) is a Poisson distribution with $\langle i-1 \rangle = \sigma_{i-1}^2 = t - s$, which localizes the integral of $x_0^+(s)$ in a window of position and width determined by i . This tells us that in order to find the qualitative shape of the age distribution $x_i^+(t)$ for $i \sim t \gg 1$, we can replace the

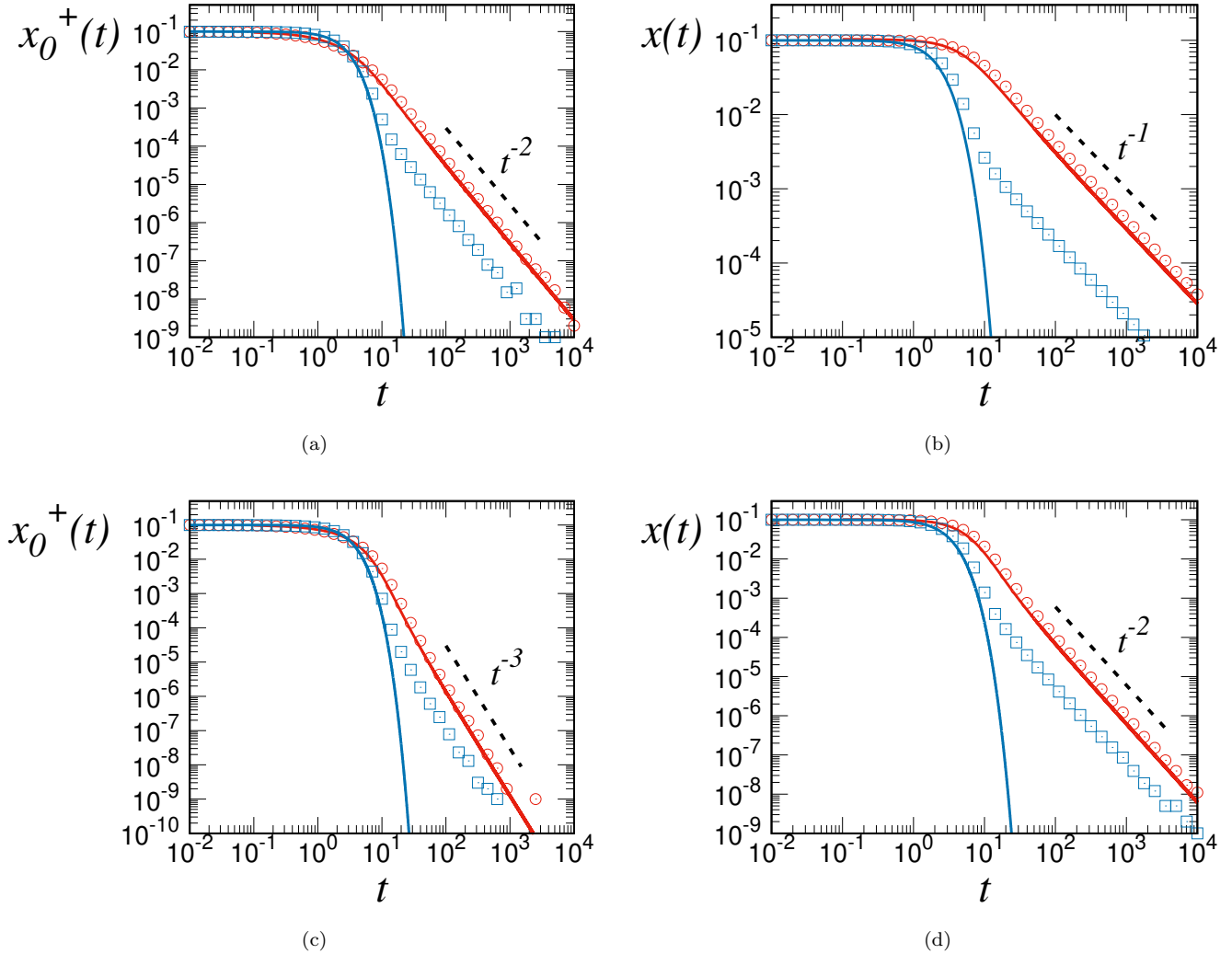


FIG. 2. Time evolution of the variables $x(t), x_0^+(t)$ for p_i given by Eq. (1) with different values of p_0, c and $p_\infty = 0$ and initial condition $x(0) = x_0^+(0) = 0.1$. Top panels are (red circles), $p_0 = 1/2, c = 2, b = 1$, and (blue squares), $p_0 = 1, c = 1, b = 1$, and bottom panels are (red circles), $p_0 = 2/3, c = 3, b = 2$, and (blue squares), $p_0 = 1, c = 2, b = 2$. Points are results from numerical simulations with $N = 10^5$ averaged over 10^4 trajectories while lines are the numerical integration of Eqs. (19,20).

early dynamics approximate solution $x_0^+(s)$ inside the integral at Eq. (18) by $x(0)e^{-(1-p_0)s}$ and $\prod_{k=0}^{i-1}(1-p_k)$ by its asymptotic expansion form $\frac{\Gamma(c)}{\Gamma(c(1-p_0))}i^{-b}$ for $i \gg 1$:

$$x_{i \gg 1}^+(t) \simeq \frac{x_0^+(0)}{t^b} \frac{\Gamma(c)}{\Gamma(c(1-p_0))} \int_0^t \frac{(t-s)^{i-1}}{(i-1)!} e^{p_0 s - t} ds. \quad (25)$$

This is essentially a function localized around $i \sim t$ whose amplitude decreases as $1/t^b$. This feature of the distribution of ages is analyzed in Fig. (3).

For $i \gtrsim 1$, however, the major contribution to the integral at Eq. (18) comes from the region $s \sim t \gg 1$ and we can use the asymptotic expression $x_0^+(s) = A s^{-(b+1)}$ as a constant inside the integral

$$x_{i \gtrsim 1}^+(t) \simeq B_i t^{-(b+1)}, \quad B_i \equiv A \prod_{k=0}^{i-1} (1-p_k), \quad (26)$$

whose validity is checked in Fig. (3).

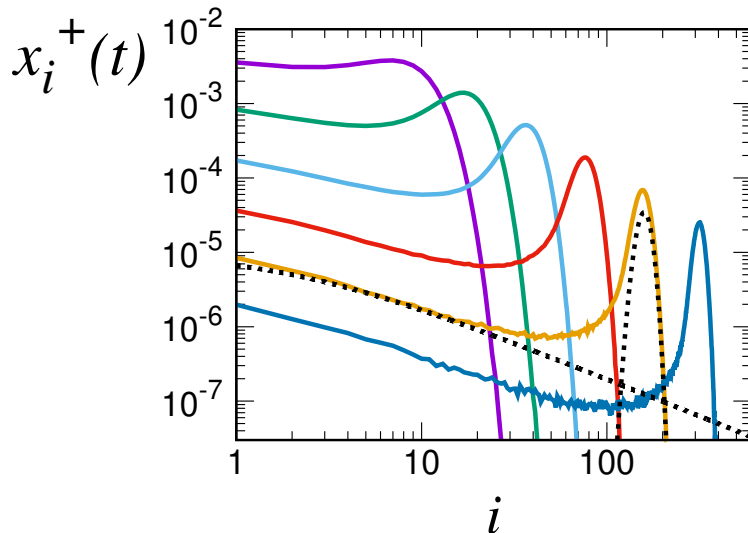


FIG. 3. Time evolution of the density of nodes in state + with age i , $x_i^+(t)$ for p_i given by Eq. (1) with $p_\infty = 0$, $p_0 = 1/2$, $c = 2$ with initial condition $x_i^+(0) = 0.1\delta_{i,0}$. Colored lines are the results of numerical simulations with $N = 10^5$ averaged over 10^4 trajectories. $x_i^+(t)$ is showed as a function of i for different snapshots $t = 10, 20, 40, 80, 160, 320$ in log-log scale. For $t = 160$ the dashed black lines are the asymptotic approximations Eqs. (25,26).

B. Aging case, Eq. (1) with $p_\infty > 0$

In this case the activation probability starts at p_0 and decays to a non-null value p_∞ . This is qualitatively similar to the case studied in [42], although in that reference the final value p_∞ was reached after a finite number of aging steps, but we do not expect this to be a significant difference.

As shown in A, $L(t)$ tends to a non-null asymptotic value $L(t \rightarrow \infty) = p_\infty$ while $G(t)$ decays exponentially:

$$G(t) \sim e^{-p_\infty t} t^{-b}, \quad b = c \frac{p_0 - p_\infty}{1 - p_\infty} \quad (27)$$

$$L(t) \sim p_\infty. \quad (28)$$

If we replace $L(t)$ by this constant value p_∞ in Eq. (20) we can use the Laplace transform $\hat{x}_0^+(s)$ of $x_0^+(t)$ to find the explicit solution:

$$\hat{x}_0^+(s) = \frac{x(0)}{s + 1 - p_\infty(1 + \hat{G}(s))} \equiv \frac{x(0)}{\hat{F}(s)}, \quad (29)$$

and from Eq. (19) we get the Laplace transform $\hat{x}(s)$ of $x(t)$:

$$\hat{x}(s) = \frac{1 + \hat{G}(s)}{\hat{F}(s)} x(0). \quad (30)$$

Note that, due to the asymptotic behavior of $G(t)$, Eq. (27), the Laplace transform $\hat{G}(s)$ does not converge for $s < -p_\infty$. It turns out that $\hat{F}(s)$ has a zero located at $s = s_1$. Hence, inverting the Laplace transform we find the asymptotic behavior $x_0^+(t) \sim x(t) \sim e^{s_1 t}$. The exact value of s_1 has to be found solving numerically $\hat{F}(s_1) = 0$ and it is found to depend non-trivially on the parameters of the model, see Figure (4a). As it is shown in this figure, we find $s_1 < 0$ for $p_0 > p_\infty$ (aging) and $s_1 > 0$ for $p_0 < p_\infty$ (anti-aging), thus the asymptotic behavior is in accordance to the linear stability analysis performed before. There are two cases where $s_1 = 0$: (i) for $p_0 = p_\infty$ which corresponds to the non-aging voter model with $x(t) = x(0)$, and (ii) for $p_\infty = 0$ where the time dependence changes from being exponential to a power law $x(t) \sim t^{-\beta}$ as explained in the previous section. The case that concern us in this section is $0 < p_\infty < p_0$, where we have $s_1 \sim -p_\infty$ for small p_∞ and as p_∞ approaches p_0 , s_1 increases until $s_1 = 0$. We have checked the proposed asymptotic behavior in the particular case $p_\infty = 0.1$, $p_0 = 0.5$, $c = 1$ in Figure 5. The theory predicts an exponential decay with $s_1 = -0.0982$ which matches perfectly compared to numerical

simulation and also compared to the numerical solution of Eqs. (19,20). In the same figure we also show the special problematic case $p_0 = 1$, with the same other parameters. In this case it is $G(t) = 0$ thus according to Eqs. (19,20) the solution is initially an exponential function as $x(t) \approx e^{-\frac{1-p_\infty}{2}t^2}$ followed by the regime $x(t) \approx e^{-(1-p_\infty)t}t^{p_0c}$. This behavior is correct in the early states of the dynamics but after it there is a crossover to a slower exponential decay $x(t) \sim e^{s_1^+ t}$. We expect this effect to be also a result of linearization, where in $x(t) = x(0)h_1(t) + x(0)^2h_2(t) + \dots$, $h_2(t)$ is slower than $h_1(t)$ which is the result that we obtained. Thus for a large enough time $t > t^*$ it can happen that $x(0)h_1(t) < x(0)^2h_2(t)$.

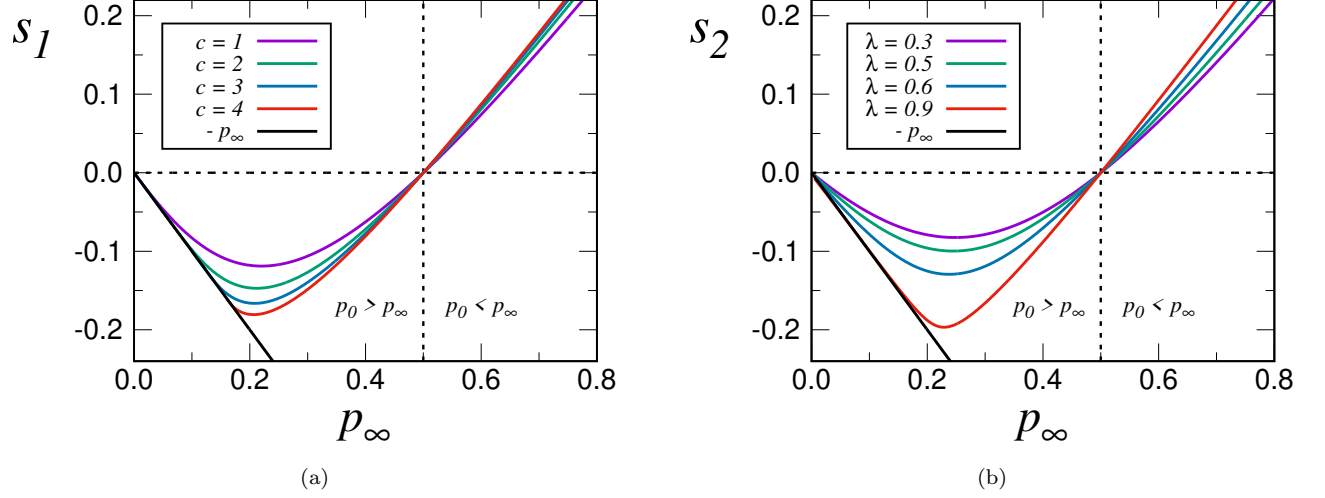


FIG. 4. Roots of the equation $\hat{F}(s) = s + 1 - p_\infty(1 + \hat{G}(s)) = 0$ as a function p_∞ with fixed $p_0 = 0.5$. The right panel is the case p_i given by Eq. (1) for different values of $c = 1, 2, 3, 4$ and in the left panel it is Eq. (2) for different values of $\lambda = 0.3, 0.5, 0.7, 0.9$. The explicit forms of the Laplace transform of G are given in A.

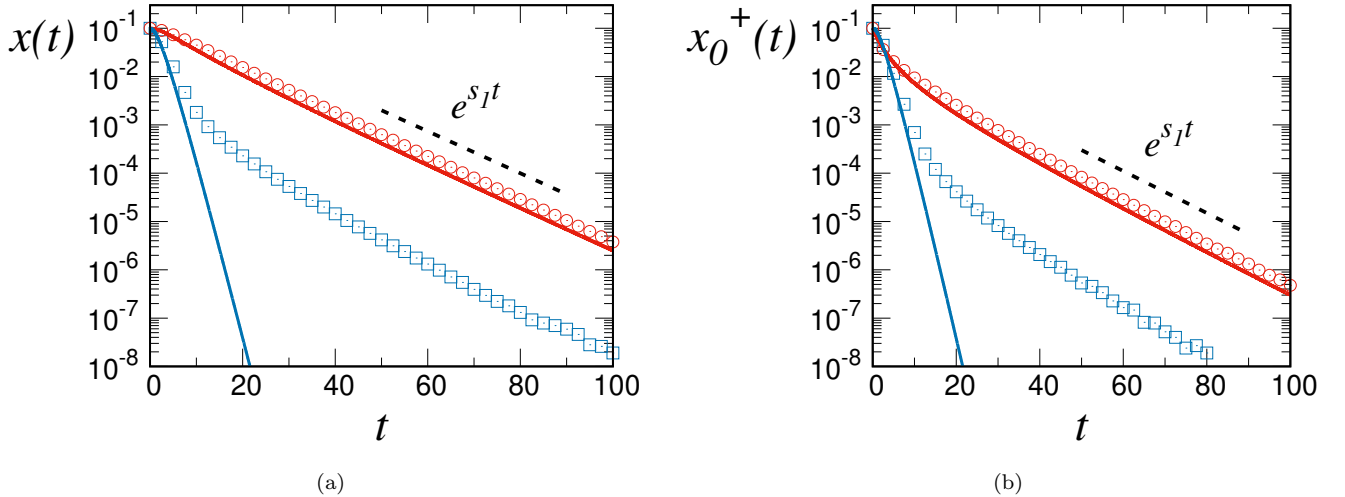


FIG. 5. Time evolution of the variables $x(t), x_0^+(t)$ for p_i given by Eq. (1) with different values of p_0, c and $p_\infty = 0.1$ and initial condition $x(0) = x_0^+(0) = 0.1$. Red circles are $p_0 = 1/2, c = 1$, and blue squares, $p_0 = 1, c = 1$. Points are results from numerical simulations with $N = 10^5$ averaged over 10^4 trajectories, while solid lines are the numerical integration of Eqs. (19,20).

C. Aging case, Eq. (2) with $p_\infty = 0$

From expression Eq. (2) in A we find the asymptotic behavior for large t

$$G(t) \sim (p_0; \lambda)_\infty, \quad (31)$$

$$L(t) = p_0 e^{-(1-\lambda)t}, \quad (32)$$

where $(a; b)_i \equiv \prod_{k=0}^{i-1} (1 - ab^k)$ is the q-Pochhammer symbol [62]. Note the remarkable property that $G(t \rightarrow \infty) \rightarrow \text{constant} > 0$ which is something that we did not observe in the other cases. As explained in B, we can solve Eqs. (19,20) in this case replacing Eqs. (31,32). Approximately, we have the exponential decay $x_0^+(t) \approx x_0(0)c_2 e^{-(1-\lambda)t}$ and $x(t)$ decays exponentially until it reaches a constant value $x(\infty) \approx x(0)c_2\lambda/p_0$ that depends on the initial condition $x(0)$. Here c_2 is a constant that depends on p_0 and λ in an intricate way, see B. In summary, the system does not order in this case. We can deduce that this will be the case as long as $G(\infty) = \prod_{k=0}^{\infty} (1 - p_k) \neq 0$ or, equivalently, if $\sum_{k=0}^{\infty} p_k$ converges. Obviously for $p_\infty \neq 0$ this is never the case, while for $p_\infty = 0$ if p_k decays faster than $p_k \sim 1/k$ the system does no order, but it does order if p_k decays slower than $p_k \sim 1/k$. The case $p_k \sim 1/k$ is somehow a critical value, where the system orders very slowly as a power law as explored in section V A. We checked this prediction against the results of numerical simulations in Figure 6 for $p_0 = 0.5$, $\lambda = 1/2$. For $p_0 = 1$ there is again the failure of the linearization, where the theory predicts that the system orders exponentially, while the numerical simulation shows the same behavior initially until a crossover is reached to a constant value $x(\infty) \neq 0$, which is smaller than in the case $p_0 \neq 1$. According to this argument $x(t) = x(0)h_1(t) + x(0)^2h_2(t) + \dots$, $h_1(\infty) = 0$ and $h_2(\infty) \neq 0$. The fixed point value is expected to scale as $x(\infty) \propto x(0)^2$ as the linear theory predicts $x(\infty) = 0$. This and the linear prediction $x(\infty) \approx c_2\lambda/p_0x(0)$ is checked with numerical simulation in Figure 7.

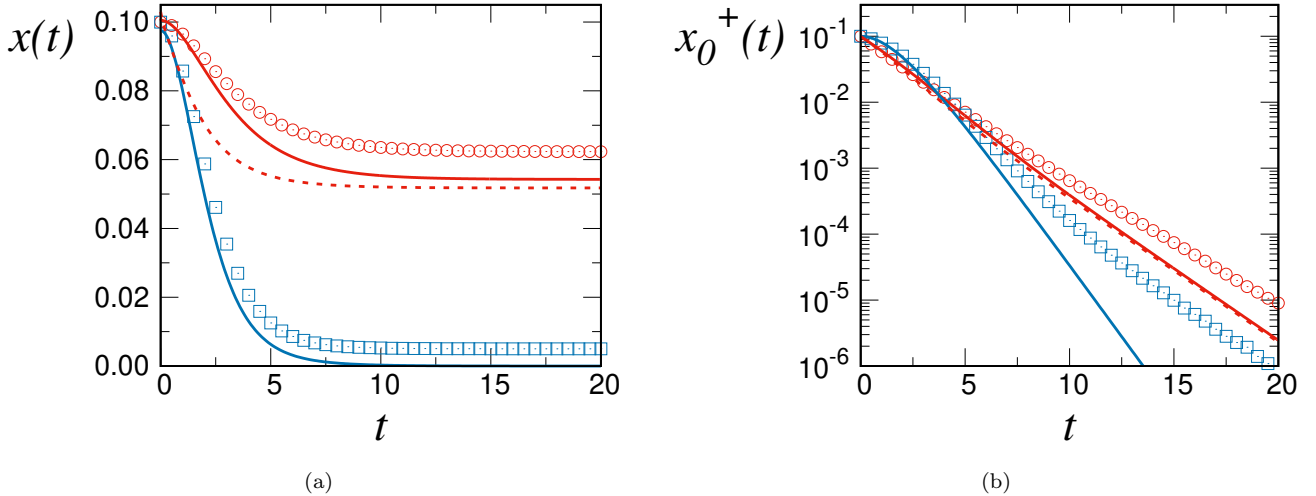


FIG. 6. Time evolution of the variables $x(t), x_0^+(t)$ for p_i given by Eq. (2) with different values of p_0, λ and $p_\infty = 0$ and initial condition $x(0) = x_0^+(0) = 0.1$. Red circles are $p_0 = 1/2, \lambda = 1/2$, and blue squares, $p_0 = 1, \lambda = 1/2$. Points are results from numerical simulations with $N = 10^5$ averaged over 10^4 trajectories, while lines are the numerical integration of Eqs. (19,20). The dashed lines are the approximate solution of B.

D. Aging case, Eq. (2) with $p_\infty > 0$

In this case, from expression Eq. (2) in A we find the asymptotic expressions

$$G(t) \sim (1 - p_\infty) \left(\frac{p_0 - p_\infty}{1 - p_\infty}; \lambda \right)_\infty e^{-p_\infty t}, \quad (33)$$

$$L(t) \sim p_\infty. \quad (34)$$

Thus, this case is similar to the one studied in section V B where $G(t)$ decays exponentially and $L(t)$ goes to a constant. Following the procedure of that section we use the Laplace transform in Eq. (19,20) after replacing $L(t)$ by its limit

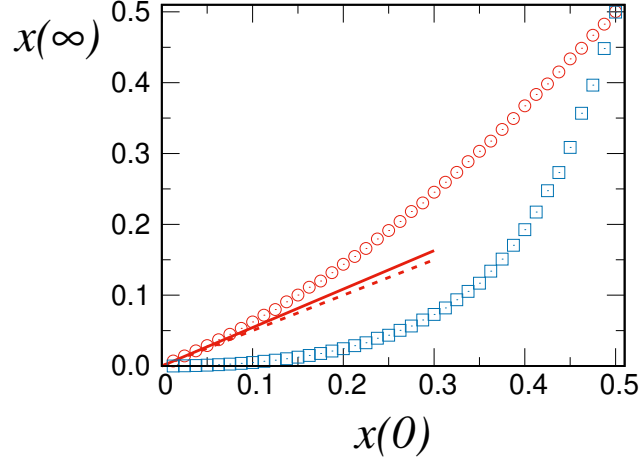


FIG. 7. Stationary value $x(\infty)$ as a function of the initial condition $x(0)$ for p_i given by Eq. (2) with $\lambda = 1/2$, $p_\infty = 0$ and $N = 10^5$. Red circles are $p_0 = 1/2$ and blue squares $p_0 = 1$, while the red line is the theoretical prediction of the linearized Eqs. (19,20), and the dashed line is the approximation of B, i.e. $x(\infty) \approx c_2 \lambda / p_0 x(0)$.

p_∞ , see A for an explicit expression for these functions. In Figure (4b) we explored the root s_2 of the denominator $\hat{F}(s)$ of Eq. (29) as a function of p_∞ . We find the same phenomenology, with $s_2 > 0$ for $p_0 < p_\infty$ and $s_2 < 0$ for $p_0 > p_\infty$, $s_2 = 0$ for $p_0 = p_\infty$ corresponding to the non-aging voter model. For $p_\infty = 0$ we also obtain $s_2 = 0$, in accordance to the result of the previous section where $x(t)$ goes to a constant. In Figure 8 we compare the results of numerical simulations of $x(t)$ with the numerical integration of Eqs. (19,20) and the asymptotic $x(t) \sim x_0^+(t) \sim e^{s_2 t}$, for $p_\infty = 0.1$, $\lambda = 0.5$, $p_0 = 0.5$ and $p_0 = 1$. The theory predicts $s_2 = -0.0616\dots$ which is in good agreement to what it is observed in the simulation. The case $p_0 = 1$ is again singular as the linear approximation fails to reproduce the long term dynamics. In the linear theory we have $G(t) = 0$ which leads to $h_1(t) \sim e^{-(1-p_\infty)t + \frac{p_0 - p_\infty}{1-\lambda}(1-e^{-(1-\lambda)t})}$. This exponential decay happens to be faster than the second order contribution, which is also exponential $h_2(t) \sim e^{s_2^* t}$, and thus for long enough time the second order prevails.

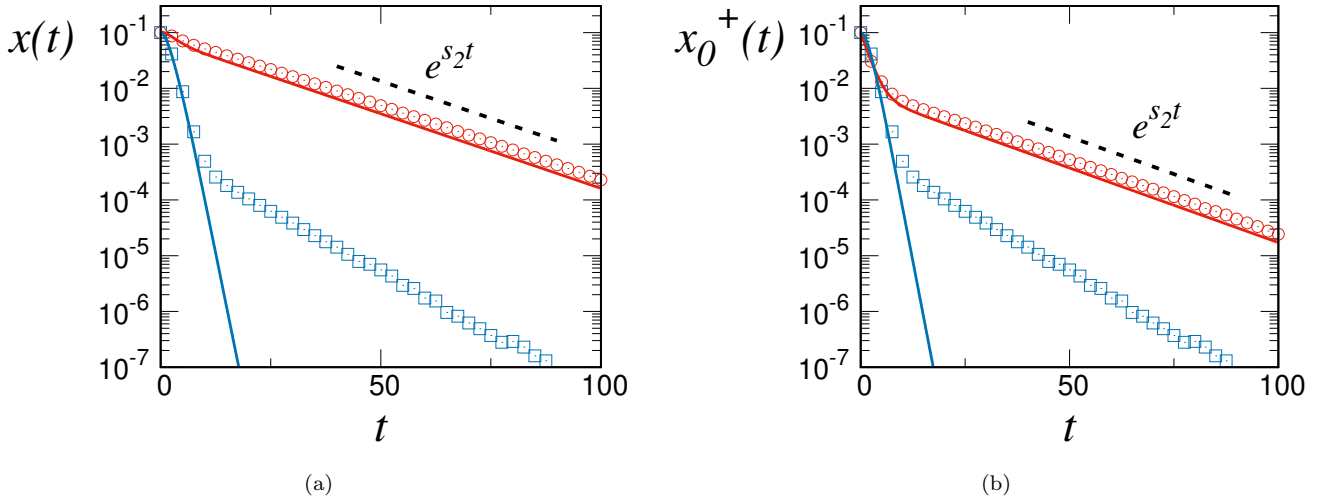


FIG. 8. Time evolution of the variables $x(t)$, $x_0^+(t)$ for p_i given by Eq. (2) with different values of p_0 , λ and $p_\infty = 0.1$, and initial condition $x(0) = x_0^+(0) = 0.1$. Red circles are $p_0 = 1/2$, $\lambda = 1/2$, and blue squares, $p_0 = 1$, $\lambda = 1/2$. Points are results from numerical simulations with $N = 10^5$ averaged over 10^4 trajectories, while lines are the numerical integration of Eqs. (19,20).

VI. SUMMARY AND CONCLUSIONS

In this work we have studied memory effects (aging and anti-aging) in an opinion dynamics model, by means of analytical and numerical approaches. More specifically, we have focused on a mean-field (all-to-all) description of the voter model, where the influence of the aging of the individuals has been modelled through the activation probability, p_i , or the copying probability of the individuals as a function of their internal age i . Overall, we have shown that the functional form of p_i has a crucial impact on how and whether the system reaches consensus or not. For the sake of concreteness, we have employed in our analysis monotonic functions p_i with three parameters: p_0 (or p_i for zero age), p_∞ (or p_i for ∞ age), and a third one, c or λ , tuning the transition $p_0 \rightarrow p_\infty$.

When the activation probability is constant $p_0 = p_\infty$, we recover the voter model. In this case, the system keeps its initial magnetization, provided the number of agents is large enough. If the activation probability is not constant and tends to a nonzero value for large ages, $p_0 \neq p_\infty > 0$, the aging and anti-aging cases produce opposite effects in the dynamics. On the one hand, for the case of aging, with $p_0 > p_\infty > 0$, the system orders with an exponential decay of the global opinion towards one of the consensus states $x \rightarrow 0, 1$. On the other hand, for the anti-aging case, with $0 < p_0 < p_\infty$, the system reaches coexistence with $x \rightarrow 1/2$.

As explained in Ref. [42], the results for $p_\infty > 0$ can be understood heuristically: the aging mechanism amplifies any small asymmetry in the initial conditions. Take an initial condition close to consensus, say $x = 0$, and all the agents with zero age. Then, the system evolves in a first, very short stage as if no aging was present since all agents have the same herding rate. After the first transitions, most of the agents become older in the state -1 , while a small fraction are younger with states ± 1 . From a dynamical point of view, the only difference between the latter situation and the voter model is in the presence of the small fraction of the young agents. In the case of aging, since the rate of changing state is bigger for the young agents, the most probable event is that a young agent copies the state of an old one. Altogether, the magnetization decreases. On the contrary, for the case of anti-aging with the young agents having smaller rates, the most probable event is that of an old copying a young. Now, the magnetization increases.

For the case of aging with zero p_∞ , $p_0 > p_\infty = 0$, the system may or may not order, depending on how “fast” is the decay of p_i to zero as the age increases. From the theoretical analysis of the integro-differential equations close to the consensus state, together with the results of numerical simulations, we infer the following criterion: if p_i decays faster than $1/i$ then the system gets trapped in a frozen state given by the initial conditions, while the system orders in other cases. The decay $p_i \sim 1/i$ can be then regarded as a critical functional form where we proved that the system orders with a power-law time dependence.

The results of $p_\infty = 0$ can also be understood using qualitative arguments. The evolution of the magnetization can be explained as for the case $p_\infty > 0$, the only difference now being the time needed for the system to reach its final value. For p_i decaying slow enough, the system reaches consensus but on a time much larger than that for $p_\infty > 0$, since it takes more time to convince all agents, specially the older ones. For the other case of p_i decaying faster, almost all agents become zealots [32] on a short time scale, and the system gets frozen on an active state, $x \neq 0, 1$, in general.

Appendix A: Asymptotic expansions

1.

If we use the expression Eq. (1) for the activation probabilities, we obtain the explicit expressions for the functions Eqs. (21,22)

$$G(t) = (1 - p_0)e^{-t} M \left(1 + c \frac{1 - p_0}{1 - p_\infty}, 1 + c, (1 - p_\infty)t \right), \quad (\text{A1})$$

$$L(t) = e^{-t} \left[p_0 M(c, c + 1, t) + t \frac{p_\infty}{1 + c} M(1 + c, 2 + c, t) \right], \quad (\text{A2})$$

where $M(\alpha, \beta, x)$ is Kummer's ${}_1F_1(\alpha; \beta; x)$ confluent hypergeometric function. Using the expansion for large z : $M(\alpha, \beta, z) \sim \frac{\Gamma(\beta)}{\Gamma(\alpha)} e^z z^{\alpha-\beta}$ we obtain in the asymptotic limit $t \rightarrow \infty$ the expansions:

$$G(t) \sim Ae^{-p_\infty t} t^{-b}, \quad (\text{A3})$$

$$L(t) \sim \frac{p_0 c}{t} + p_\infty, \quad (\text{A4})$$

$$A = (1 - p_\infty) \frac{\Gamma(c)}{\Gamma\left(c \frac{1-p_0}{1-p_\infty}\right)}, \quad (\text{A5})$$

$$b = c \frac{p_0 - p_\infty}{1 - p_\infty}. \quad (\text{A6})$$

The expressions for $G(t)$ assume $p_\infty \neq 1$. For $p_\infty = 1$ we find

$$G(t) = \Gamma(c)(c(1-p_0))^{1-c/2} e^{-t} t^{-c/2} I_c\left(2\sqrt{c(1-p_0)t}\right) \quad (\text{A7})$$

$$\sim \frac{\Gamma(c)}{\sqrt{2\pi\sqrt{2}}} [c(1-p_0)]^{(3-2c)/4} t^{-(c+2)/4} e^{-t}. \quad (\text{A8})$$

It is also possible to obtain the Laplace transform of $G(t)$ as:

$$\hat{G}(s) = \frac{1-p_0}{1+s} {}_2F_1\left[1, 1+c \frac{1-p_0}{1-p_\infty}; 1+c; \frac{1-p_\infty}{1+s}\right]. \quad (\text{A9})$$

2.

In the case of activation probabilities given by Eq. (2) it is possible to obtain $L(t)$ analytically:

$$L(t) = (p_0 - p_\infty) e^{-(1-\lambda)t} + p_\infty, \quad (\text{A10})$$

although we have not been able to find a closed expression for $G(t)$,

$$G(t) = e^{-t} \sum_{i=0}^{\infty} \frac{(1-p_\infty)^{i+1} \left(\frac{p_0-p_\infty}{1-p_\infty}; \lambda\right)_{i+1}}{i!} t^i, \quad (\text{A11})$$

with $(q; a)_n$ the q-Pochhammer symbol. It is possible, however, to obtain the asymptotic expansion for $t \rightarrow \infty$ as

$$G(t) \sim (1-p_\infty) \left(\frac{p_0-p_\infty}{1-p_\infty}; \lambda\right)_\infty e^{-p_\infty t}. \quad (\text{A12})$$

In the particular case $p_\infty = 0$ it yields $G(t) \sim (p_0; \lambda)_\infty$.

Finally, we mention the Laplace transform of $G(t)$ as:

$$\hat{G}(s) = \sum_{i=0}^{\infty} \left(\frac{1-p_\infty}{1+s}\right)^{i+1} \left(\frac{p_0-p_\infty}{1-p_\infty}; \lambda\right)_{i+1}. \quad (\text{A13})$$

For the numerical calculation of $G(t)$ and $\hat{G}(s)$ in this case we use Eqs.(A11,A13) using a sufficiently large number of terms in the sums.

Appendix B: Solution of Eqs. (19,20) using Eqs. (31,32)

If $G(t) \equiv G_\infty$ is a constant, we can differentiate Eq. (19) and obtain a system of differential equations:

$$\frac{dx}{dt} = \frac{dx_0^+}{dt} + G_\infty x_0^+(t), \quad (\text{B1})$$

$$\frac{dx_0^+}{dt} = -x_0^+ + L(t)x(t). \quad (\text{B2})$$

From the last equation we get $x(t) = \left(\frac{dx_0^+}{dt} + x_0^+\right) / L(t)$ which, replaced in Eq.(B1) leads to a closed second order linear differential equation for $x_0^+(t)$. The change of variables $z \equiv -\frac{p_0}{1-\lambda}e^{-(1-\lambda)t}$ makes the coefficients of the equation to be simple polynomials and a standard technique based of Frobenius power-series expansion leads to the general solution $x(t) = [c_1x^{(1)}(t) + c_2x^{(2)}(t)]x(0)$, $x_0^+(t) = [c_1x_0^{(1)}(t) + c_2x_0^{(2)}(t)]x(0)$, where c_1 and c_2 are constants imposed by satisfying the initial condition $x(0) = x_0^+(0) = 1$, and

$$x_0^{(1)}(t) = e^{-t}M\left(\frac{1-G_\infty}{1-\lambda}, \frac{1}{1-\lambda}, -\frac{p_0}{1-\lambda}e^{-(1-\lambda)t}\right), \quad (\text{B3})$$

$$x_0^{(2)}(t) = e^{-(1-\lambda)t}M\left(1 - \frac{G_\infty}{1-\lambda}, \frac{1-2\lambda}{1-\lambda}, -\frac{p_0}{1-\lambda}e^{-(1-\lambda)t}\right), \quad (\text{B4})$$

$$x^{(1)}(t) = (1-G_\infty)e^{-t}M\left(1 + \frac{1-G_\infty}{1-\lambda}, \frac{2-\lambda}{1-\lambda}, -\frac{p_0}{1-\lambda}e^{-(1-\lambda)t}\right), \quad (\text{B5})$$

$$x^{(2)}(t) = \frac{\lambda}{p_0}M\left(1 - \frac{G_\infty}{1-\lambda}, \frac{1-2\lambda}{1-\lambda}, -\frac{p_0}{1-\lambda}e^{-(1-\lambda)t}\right) + \quad (\text{B6})$$

$$\frac{1-\lambda-G_\infty}{1-2\lambda}e^{-(1-\lambda)t}M\left(2 - \frac{G_\infty}{1-\lambda}, \frac{2-3\lambda}{1-\lambda}, -\frac{p_0}{1-\lambda}e^{-(1-\lambda)t}\right). \quad (\text{B7})$$

In the limit $t \rightarrow \infty$, the asymptotic behavior is

$$x_0^{(1)}(t) \rightarrow e^{-t}, \quad (\text{B8})$$

$$x_0^{(2)}(t) \rightarrow e^{-(1-\lambda)t}, \quad (\text{B9})$$

$$x^{(1)}(t) \rightarrow (1-G_\infty)e^{-t}, \quad (\text{B10})$$

$$x^{(2)}(t) \rightarrow \frac{\lambda}{p_0}, \quad (\text{B11})$$

leading to

$$x_0^+(t) \rightarrow x(0)c_2e^{-(1-\lambda)t}, \quad (\text{B12})$$

$$x(t) \rightarrow x(0)c_2\frac{\lambda}{p_0}. \quad (\text{B13})$$

We do not reproduce the explicit expressions for the constants c_1 and c_2 as they are too long and not very illuminating. It suffices to say that in the case $\lambda = 1/2$, $p_0 = 1/2$ used in subsection V C it is $c_2 = 1/2$.

ACKNOWLEDGEMENTS

Partial financial support has been received from the Agencia Estatal de Investigacion (AEI, Spain) and Fondo Europeo de Desarrollo Regional under Project PACSS RTI2018-093732-B-C21 (AEI/FEDER,UE) and the Spanish State Research Agency, through the Maria de Maeztu Program for units of Excellence in R&D (MDM-2017-0711). A. F. P. acknowledges support by the Formacion de Profesorado Universitario (FPU14/00554) program of Ministerio de Educacion, Cultura y Deportes (MECD) (Spain). We thank J. F. Gracia for valuable discussions concerning the results of Ref. [41].

REFERENCES

-
- [1] R. Pastor-Satorras, A. Vespignani, Epidemic spreading in scale-free networks, *Physical review letters* 86 (14) (2001) 3200.
 - [2] R. Pastor-Satorras, C. Castellano, P. Van Mieghem, A. Vespignani, Epidemic processes in complex networks, *Reviews of modern physics* 87 (3) (2015) 925.
 - [3] D. M. Abrams, S. H. Strogatz, Linguistics: Modelling the dynamics of language death, *Nature* 424 (6951) (2003) 900.
 - [4] X. Castelló, V. M. Eguíluz, M. San Miguel, Ordering dynamics with two non-excluding options: bilingualism in language competition, *New Journal of Physics* 8 (12) (2006) 308.

- [5] D. Stauffer, X. Castelló, V. M. Eguiluz, M. San Miguel, Microscopic Abrams–Strogatz model of language competition, *Physica A: Statistical Mechanics and its Applications* 374 (2) (2007) 835–842.
- [6] F. Vazquez, X. Castelló, M. S. Miguel, Agent based models of language competition: Macroscopic descriptions and order-disorder transition, *J. Stat. Mech. Theory Exp* 2010.
- [7] A. Kirman, Ants, rationality, and recruitment, *Quart. J. Econ* 108 (1993) 137.
- [8] S. Alfarano, T. Lux, F. Wagner, Time Estimation of agent-based models: The case of an asymmetric Herding model, *Comput. Econ* 26 (2005) 19.
- [9] S. Alfarano, T. Lux, F. Wagner, Time variation of higher moments in a financial market with heterogeneous agents: An analytical approach, *Econ. Dyn. Control* 32 (2008) 101.
- [10] S. Alfarano, M. Milaković, Network structure and N-dependence in agent-based herding models, *Journal of Economic Dynamics and Control* 33 (2009) 78.
- [11] V. Gontis, A. Kononovicius, Spurious Memory in Non-Equilibrium Stochastic Models of Imitative Behavior, *Entropy* 19 (2017) 387.
- [12] A. Carro, R. Toral, M. San Miguel, Markets, Herding and Response to External Information, *PloS one* 10 (7) (2015) e0133287.
- [13] A. Kononovicius, J. Ruseckas, Order book model with herd behavior exhibiting long-range memory, *Physica A: Statistical Mechanics and its Applications* 525 (2019) 171 – 191.
- [14] A. Barrat, M. Barthelemy, A. Vespignani, *Dynamical processes on complex networks*, Cambridge university press, 2008.
- [15] C. Castellano, S. Fortunato, V. Loreto, Statistical physics of social dynamics, *Reviews of modern physics* 81 (2) (2009) 591.
- [16] J. Fernández-Gracia, K. Suchecki, J. J. Ramasco, M. San Miguel, V. M. Eguiluz, Is the Voter Model a Model for Voters?, *Phys. Rev. Lett.* 112 (2014) 158701.
- [17] P. Clifford, A. Sudbury, A model for spatial conflict, *Biometrika* 60 (3) (1973) 581–588.
- [18] R. A. Holley, T. M. Liggett, Ergodic theorems for weakly interacting infinite systems and the voter model, *The annals of probability* 3 (4) (1975) 643–663.
- [19] F. Vazquez, V. M. Eguiluz, Analytical solution of the voter model on uncorrelated networks, *New Journal of Physics* 10 (6) (2008) 063011.
- [20] S. Redner, Reality Inspired Voter Models: A Mini-Review, arXiv e-prints (2018) arXiv:1811.11888.
- [21] P. L. Krapivsky, S. Redner, E. Ben-Naim, *A kinetic view of statistical physics*, Cambridge University Press, 2010.
- [22] T. M. Liggett, *Interacting particle systems*, vol. 276, Springer Science & Business Media, 2012.
- [23] A. F. Peralta, A. Carro, M. S. Miguel, R. Toral, Stochastic pair approximation treatment of the noisy voter model, *New Journal of Physics* 20 (2018) 103045.
- [24] A. Carro, R. Toral, M. S. Miguel, The noisy voter model on complex networks, *Scientific Reports* 6 (2016) 24775.
- [25] P. Nyczka, K. Sznajd-Weron, J. Cislo, Phase transitions in the q -voter model with two types of stochastic driving, *Phys. Rev. E* 86 (2012) 011105.
- [26] P. Nyczka, K. Sznajd-Weron, Anticonformity or Independence?—Insights from Statistical Physics, *Journal of Statistical Physics* 151 (1) (2013) 174–202.
- [27] A. Jędrzejewski, Pair approximation for the q -voter model with independence on complex networks, *Phys. Rev. E* 95 (2017) 012307.
- [28] A. F. Peralta, A. Carro, M. S. Miguel, R. Toral, Analytical and numerical study of the non-linear noisy voter on complex networks, *Chaos* 28 (2018) 075516.
- [29] A. R. Vieira, C. Anteneodo, Threshold q -voter model, *Phys. Rev. E* 97 (2018) 052106.
- [30] T. Raducha, B. Min, M. S. Miguel, Coevolving nonlinear voter model with triadic closure, *EPL (Europhysics Letters)* 124 (3) (2018) 30001.
- [31] B. Min, M. S. Miguel, Multilayer coevolution dynamics of the nonlinear voter model, *New Journal of Physics* 21 (3) (2019) 035004.
- [32] N. Khalil, M. S. Miguel, R. Toral, Zealots in the mean-field noisy voter model, *Physical Review* 97.
- [33] N. Khalil, R. Toral, The noisy voter model under the influence of contrarians, *Physica A* 515 (2019) 81–92.
- [34] A. Jędrzejewski, K. Sznajd-Weron, Impact of memory on opinion dynamics, *Physica A: Statistical Mechanics and its Applications* 505 (2018) 306 – 315.
- [35] B. Min, K. i. Goh, I. m. Kim, Suppression of epidemic outbreaks with heavy-tailed contact dynamics, *Europhys. Lett* 103 (2013) 50002.
- [36] M. Boguñá, L. Lafuerza, R. Toral, M. Á. Serrano, Simulating non-Markovian stochastic processes, *Physical Review E* 90 (2014) 042108.
- [37] M. Starnini, J. P. Gleeson, M. Boguñá, Equivalence between Non-Markovian and Markovian Dynamics in Epidemic Spreading Processes, *Phys. Rev. Lett* 118 (2017) 128301.
- [38] S. P. Blythe, R. M. Anderson, Variable Infectiousness in HIV Transmission Models, *Math. Med. Biol* 5 (1988) 181.
- [39] N. G. van Kampen, Remarks on Non-Markov Processes, *Braz. J. Phys* 28 (1998) 90.
- [40] J. Lucza, Non-markovian stochastic processes: Colored noise, *Chaos* 15 (2005) 026107.
- [41] J. Fernández-Gracia, V. M. Eguiluz, M. San Miguel, Update rules and interevent time distributions: Slow ordering versus no ordering in the voter model, *Physical Review E* 84 (1) (2011) 015103.
- [42] H.-U. Stark, C. J. Tessone, F. Schweitzer, Decelerating Microdynamics Can Accelerate Macrodynamics in the Voter Model, *Phys. Rev. Lett* 101 (2008) 018701.

- [43] E. Ben-Naim, L. Frachebourg, P. L. Krapivsky, Coarsening and persistence in the voter model, *Physical Review E* 53 (4) (1996) 3078.
- [44] V. Sood, S. Redner, Voter model on heterogeneous graphs, *Physical review letters* 94 (17) (2005) 178701.
- [45] K. Suchecki, V. M. Eguíluz, M. San Miguel, Voter model dynamics in complex networks: Role of dimensionality, disorder, and degree distribution, *Physical Review E* 72 (3) (2005) 036132.
- [46] O. Artime, A. F. Peralta, R. Toral, J. J. Ramasco, M. S. Miguel, Aging-induced phase transition, *Phys. Rev. E* 98 (2018) 032104.
- [47] O. Artime, A. Carro, A. F. Peralta, J. J. Ramasco, M. San Miguel, R. Toral, Herding and idiosyncratic choices: Nonlinearity and aging-induced transitions in the noisy voter model, arXiv e-prints arXiv:1812.05378.
- [48] D. Considine, S. Redner, H. Takayasu, Comment on “Noise-induced bistability in a Monte Carlo surface-reaction model”, *Phys. Rev. Lett.* 63 (1989) 2857–2857.
- [49] B. L. Granovsky, N. Madras, The noisy voter model, *Stoch. Proc. Appl* 55 (23).
- [50] Y. Wu, C. Zhou, J. Xiao, J. Kurths, H. J. Schellnhuber, Evidence for a bimodal distribution in human communication, *PNAS* 107 (2010) 18803.
- [51] J. Candia, M. C. González, P. Wang, T. Schoenharl, G. Madey, A. Barabási, Uncovering individual and collective human dynamics from mobile phone records, *J. Phys. A: Math. Theor* 41 (2008) 224015.
- [52] T. Pérez, K. Klemm, V. M. Eguíluz, Competition in the presence of aging: dominance, coexistence, and alternation between states, *Sci. Rep* 6 (2016) 21128.
- [53] O. Artime, J. J. Ramasco, M. S. Miguel, Dynamics on networks: competition of temporal and topological correlations, *Sci. Rep* 7 (2017) 41627.
- [54] O. Artime, J. F. Gracia, J. J. Ramasco, M. S. Miguel, Joint effect of ageing and multilayer structure prevents ordering in the voter model, *Sci. Rep* 7 (2017) 7166.
- [55] D. Escaff, R. Toral, C. Van Den Broeck, K. Lindenberg, A continuous-time persistent random walk model for flocking, *Chaos* 28 (7) (2018) 075507.
- [56] O. Artime, N. Khalil, R. Toral, M. S. Miguel, First-passage distributions for the one-dimensional Fokker-Planck equation, *Physical Review* 98.
- [57] N. van Kampen, *Stochastic Processes in Physics and Chemistry*, North-Holland, Amsterdam, third edn., 2007.
- [58] R. Toral, P. Colet, *Stochastic Numerical Methods: An Introduction for Students and Scientists*, Wiley, URL <http://eu.wiley.com/WileyCDA/WileyTitle/productCd-3527411496.html>, 2014.
- [59] A. F. Peralta, R. Toral, System-size expansion of the moments of a master equation, *Chaos* 28 (2018) 106303.
- [60] J. Ozaita, Noisy voter model with partial aging and anti-aging, Master’s thesis, University of the Balearic Islands, Palma, Spain, 2018.
- [61] J. T. Day, Note on the Numerical Solution of Integro-Differential Equations, *The Computer Journal* 9 (4) (1967) 394–395.
- [62] URL https://en.wikipedia.org/wiki/Q-Pochhammer_symbol, 2019.